

Self-organizing maps for geoscientific data analysis: geological interpretation of multidimensional geophysical data

Christian D. Klose

Received: 28 August 2004 / Revised: 3 November 2005 / Accepted: 15 December 2005 / Published online: 29 July 2006
© Springer Science + Business Media B.V. 2006

Abstract Data interpretation is a common task in geoscientific disciplines. Interpretation difficulties occur especially if the data that have to be interpreted are of arbitrary dimension. This paper describes the application of a statistical method, called self-organizing mapping (SOM), to interpret multidimensional, non-linear, and highly noised geophysical data for purposes of geological prediction. The underlying theory is explained, and the method is applied to a six-dimensional seismic data set. Results of SOM classifications can be represented as two-dimensional images, called feature maps. Feature maps illustrate the complexity and demonstrate interrelations between single features or clusters of the complete feature space. SOM images can be visually described and easily interpreted. The advantage is that the SOM method considers interdependencies between all geophysical features at each instance. An application example of an automated geological interpretation based on the geophysical data is shown.

Keywords geological interpretation · multidimensional geophysical data · neural information processing · self-organizing mapping

1. Introduction and objectives

The interpretation of multidimensional geophysical data generated during geological exploration and used for predictive modelling (e.g., underground mining and oil/gas exploration) is a challenging task in applied geophysics. For instance, the prediction of small-scale geotechnical hazardous structures is difficult with surface-based methods during deep underground tunnel excavations. For that purpose, a series of seismic measurements has been conducted in the granitic gneisses of the Penninic gneiss zone along the 2600-m-long and up to 1400-m-deep Faïdo access tunnel, an adit to the 57-km-long Gotthard base tunnel in Switzerland [1]. The goal of this study is to detect and later interpret seismic features (e.g., seismic velocities), which are significantly related to geological features (e.g., fracture length). An automated seismic interpretation system will be used for geological prediction within planned and still unexcavated tunnel segments to mitigate the risk during the underground excavation process.

Geophysical data have been acquired from scanlines within tomograms and from seismograms that were obtained from selected wall sections in the Faïdo tunnel. Two-dimensional tomograms image the interior of the elastic rock mass properties surrounding the tunnel, whereas seismograms represent the amplitude records of the acoustic waves that are generated during the in situ measurements. Geological features result from observations and descriptions along the tunnel sections.

Generally, the disadvantage of seismic data, measured under in situ conditions, is that the seismic features vary randomly within the rock mass, in contrast to laboratory experiments [2] and theoretical modelling [3–6] where parameters can be kept unchanged.

C. D. Klose
Department of Geoengineering, GeoForschungsZentrum,
14473 Potsdam, Germany

C. D. Klose (✉)
Lamont-Doherty Earth Observatory,
PO Box 1000, Palisades NY 10964, USA
e-mail: cklose@gfz-potsdam.de

Additionally, they are complex, highly noised, and non-linearly related to the geology. In selected field studies [7, 8], geophysical data are interpreted by conventional methods such as profiling or correlations. In such cases, geophysical and geological features are compared and evaluated pairwise (feature by feature). Thus, interpretations become difficult, which may lead to ambiguous interpretation results.

This study is built on an approach that employs neural information processing to characterize the geology of the granitic gneisses from all jointly used seismic rock mass features. The principle method is termed self-organizing maps (SOM) and was first introduced by [9, 10]. Interpretations are based on six-dimensional seismic feature vectors that consist of the compression-wave and shear-wave velocities (v_p , v_s), the dynamic Poisson's ratio (ν), the shear-wave anisotropy (ξ), and, additionally, the shape measure (S) and shape intensity (I) of the polarization ellipsoids of the leading shear waves [1].

The paper is organized as follows. Section 2 introduces the theory of the SOM and explains different ways of interpreting SOM images by single features and feature clusters. Section 3 outlines and discusses the results of the SOM classification and describes an application example outlined in an unknown region close to the Faido tunnel (Switzerland). Finally, Section 4 gives a short conclusion.

2. Methods

2.1. Theoretical background

Self-organizing maps, introduced by Kohonen [9, 10], are simple analogues to the brain's way to organize

information in a logical manner. The main purpose of this neural information processing is the transformation of a feature vector of arbitrary dimension drawn from the given feature space into simplified generally two-dimensional discrete maps. A SOM network performs the transformation adaptively in a topological ordered fashion. This type of neural network utilizes an unsupervised learning method, known as competitive learning, and is useful for analysing data with unknown relationships. A SOM neural network is structured in two layers: an input layer and a Kohonen layer (Figure 1A). The Kohonen layer represents a structure with a single two-dimensional map consisting of neurons arranged in rows and columns. Each neuron of this discrete lattice is fixed and is fully connected with all source neurons in the input layer.

If a single neuron in the Kohonen layer is excited by some stimulus, neurons in the surrounding area are also excited. That means for the given task of interpreting multidimensional geophysical data, each seismic feature vector \vec{x} , which is presented to the six neurons of the input layer, typically causes a localized region of active neurons against the quiet background in the Kohonen layer. The degree of lateral interaction between a stimulated neuron $j(\vec{x})$ and neighbouring neurons is usually described by a *Gaussian function* (Figure 1B):

$$h_{k,j(\vec{x})} = \exp\left(-\frac{d_{k,j(\vec{x})}^2}{2\sigma^2}\right). \quad (1)$$

d is the lateral neuron distance in the Kohonen layer, σ is the *effective width* that changes during the learning process, and h is the activity of the neighbouring

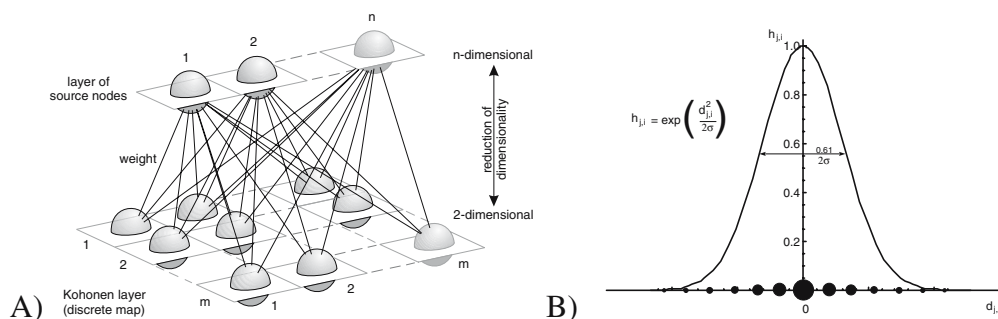


Figure 1 (A) Illustration of an SOM neural network. The SOM projects the information of an n -dimensional feature space into a two-dimensional lattice of neurons, whereby the dimensions are reduced. n (seismic) features of a feature vector, also called input vector, $\{v_p, v_s, \nu, \xi, S, I\}$, are represented to n source nodes. After training and classification, the feature vectors can be seen

in the Kohonen lattice as active neurons. The Kohonen layer typically consists of a localized region of active neurons against the quiet background. The size of the black spheres in picture (B) shows the neuron activities. The degree of lateral interaction between stimulated neuron and neighboring neurons is usually described by a *Gaussian function*.

neurons. Feature vectors occur in the Kohonen layer in the same topological order as they are presented by the metric (similarity) relations in the original feature space, while performing a dimensionality reduction of the original feature space.

Before the self-organizing procedure begins, the link values, called weights,

$$\vec{w}_k = \{w_{(k,v_p)}, w_{(k,v_s)}, w_{(k,v)}, w_{(k,\xi)}, w_{(k,S)}, w_{(k,I)}\}^T \quad (2)$$

are initialized as random values. \vec{w}_k connects the n input layer neurons to the l neurons in the Kohonen layer. n is the dimension of the input space (seismic feature space: $\{v_p, v_s, v, \xi, S, I\}$), and l is the number of all Kohonen neurons with $k = 1, 2, \dots, m, \dots, l$.

Learning occurs during the self-organizing procedure as feature vectors

$$\vec{x} = \{v_p, v_s, v, \xi, S, I\}^T, \quad (3)$$

also called input vectors, are presented to the input layer of the network. The neurons of the Kohonen layer compete to see which neuron will be stimulated by the feature vector \vec{x} . The weights \vec{w}_k are used to determine only one stimulated neuron in the Kohonen layer after the *winner-takes-all* principle. This principle can be summarized as follows: for each \vec{x} , the Kohonen neurons compute their respective values of a discriminant function (i.e., Euclidean distance $\|\vec{x}_i - \vec{w}_k\|$). These values are used to define the winner neuron. That means the network determines the index j of that neuron, whose weight \vec{w}_k is the closest to vector \vec{x}_i by

$$j(\vec{x}_i) = \arg \min_k \|\vec{x}_i - \vec{w}_k\| \quad | \quad k = 1, 2, \dots, m, \dots, l. \quad (4)$$

The particular neuron is declared winner of the competition. Afterwards, the learning procedure modifies the weights \vec{w}_j of the winner neuron and the winners neighbourhood.

$$\vec{w}_k(t + 1) = \vec{w}_k(t) + \eta(t) h_{k,j(\vec{x})}(t) (\vec{x}_i(t) - \vec{w}_k(t)), \quad (5)$$

where $\eta(t)$ is the learning-rate parameter during the calculation step t , and $h_{k,j(\vec{x})}(t)$ is the neighbourhood function centred around the winning neuron $j(\vec{x}_i)$. The neighbourhood function or *Gaussian function* determines how much the neighbouring neurons become modified (Equation 1 and Figure 1B). Neurons within the winners neighbourhood participate in the learning

process. During the self-organizing process, the neighbourhood size σ decreases until its size is zero. In this case, only the winning neuron is modified each time an input vector is presented to the network. The learning rate η – the amount each weight can be modified – decreases during the learning as well. Once the SOM algorithm has converged, two-dimensional feature maps of Kohonen neurons display the following important statistical characteristics of the represented feature space [10].

Property 1. Approximation: A feature map represented by a set of weights in the Kohonen layer provides a good approximation to the input space.

Property 2. Topological ordering: The two-dimensional feature map is topologically ordered in the sense that similar Kohonen layer neurons correspond to similar feature vectors of the higher dimensional input space.

Property 3. Density matching: The feature map reflects variations in the statistics of the distribution of the original feature space: regions in the input space from which sample vectors are drawn with a high probability of occurrence are mapped onto larger domains in the Kohonen layer, and therefore with better resolution than regions in the input space where sample vectors are drawn with a low probability of occurrence.

An SOM neural network is trained when, on each location along the seismic profiles, a feature vector $\vec{x}_i = \{v_p, v_s, v, \xi, S, I\} \mid i = 1, 2, 3, \dots, 729$ is drawn and presented to the SOM network. The memory of the trained network is finally based on 729 six-dimensional seismic feature vectors. The structure and network parameters can be described as follows:

represented feature space:	\mathbb{R}^6	$\{v_p, v_s, v, \xi, S, I\}^T$
number of input neurons n :	6	
number of feature/input vectors:	729	in situ data
number of Kohonen neurons m :	100	(10 by 10 lattice)
number of weights l :	600	
number of iterations t_F :	5000	
initial learning rate $\eta(t = 0)$:	0.5	
final learning rate $\eta(t_F)$:	0.01	
initial neighbourhood size $\sigma(t = 0)$:	5	
final neighbourhood size $\sigma(t_F)$:	1	decreasing every 1000 iterations

2.2. Mapping of single features

After the learning procedure is finished, the stored information of the six-dimensional seismic feature space can be visualized as the two-dimensional feature maps of the Kohonen layer. Again, each \vec{x}_i that is presented to the trained network stimulates a specific neuron in the Kohonen layer. The network determines the index j of that neuron, whose weight \vec{w}_k is closest to vector \vec{x}_i by

$$j(\vec{x}_i) = \arg \min_k \|\vec{x}_i - \vec{w}_k\| \quad | \quad k = 1, 2, \dots, 100. \quad (6)$$

Neuron j represents \vec{x}_i as best as possible and becomes active in the Kohonen layer (Figure 2). For each active neuron that is related to \vec{x}_i , single seismic or geological features can be imaged as a single component plane [12] within the Kohonen layer. Therefore, each feature is divided into four classes or logic sets: *very low* (v.l.), *low* (l.), *high* (h.), and *very high* (v.h.). The definition of the classes was based on the probability density kernels of each feature (Figures 3 and 4). The kernel densities were determined by a non-parametric technique of probability density estimation [13]. Classes

instead of real values were used, only due to practical reasons of communication between cross-disciplinary co-workers on the building site of the Faido tunnel. It is easier to understand; for example, the shear-wave velocity is *very low* than v_s , which is 2.6 km/s, especially when the relations between the features are unknown and the feature spaces are highly noised. The class boundaries result from the descriptive kernel parameters: minimum (Min), first quartile ($P_{25\%}$), second quartile ($P_{50\%}$), third quartile ($P_{75\%}$), and maximum (Max). The geological features are latent (to interpreted) variables. They can also be visualized in the SOM feature maps, but they do not build up the stored information of the SOM feature maps.

2.3. Mapping of feature clusters

This approach shows differences between homogeneous units (clusters) within the rock mass along the tunnel from a global perspective, whereas six seismic and eight geological features built up 14-dimensional vectors \vec{y} . The eight geological rock mass features are uniaxial compressive strength of the rock σ_c , water flow

Figure 2 Classification scheme of an SOM neural network. Six-dimensional seismic feature vectors \vec{x} were drawn along a seismic profile in the tunnel (here, profile 2360–2433 m). Several tunnel locations can be seen: 2380, (2386), 2394, (2402), 2406, and 2422 m. Every \vec{x} is presented to the network. The classification is done when a neuron in the Kohonen lattice (right, top) is stimulated. This neuron is active (black) and can be imaged in the lattice (right, bottom). All active neurons that can be seen are related to every \vec{x} . The white trace in the black region (right, bottom) shows schematically which neurons become active when the profile (left) is being crossed.

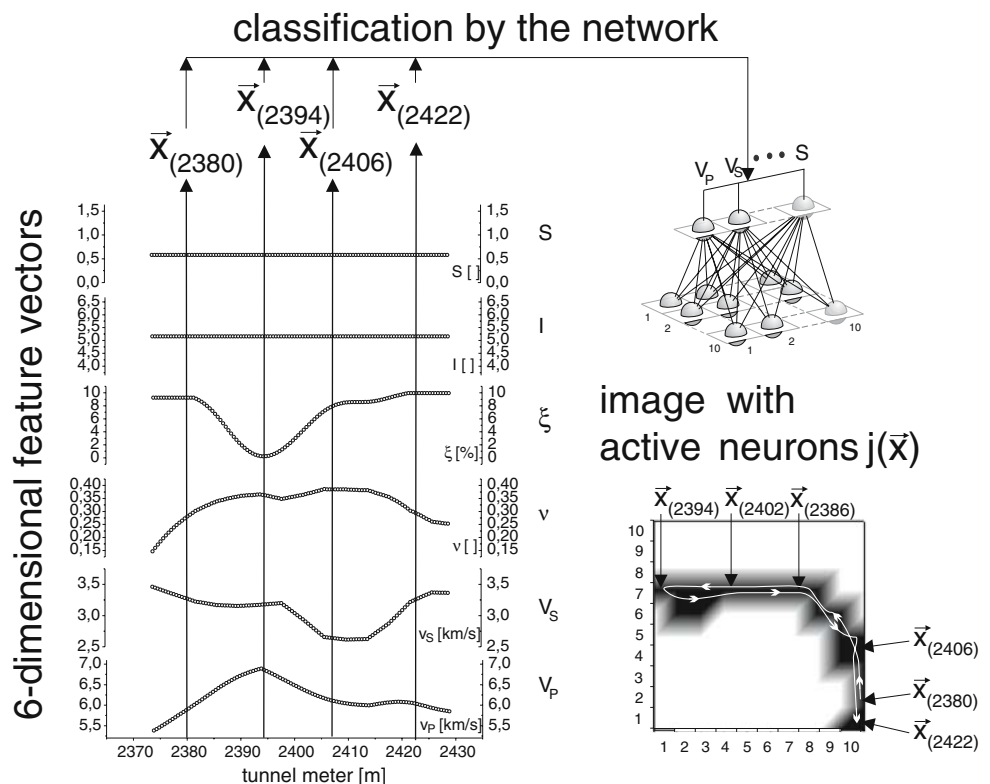
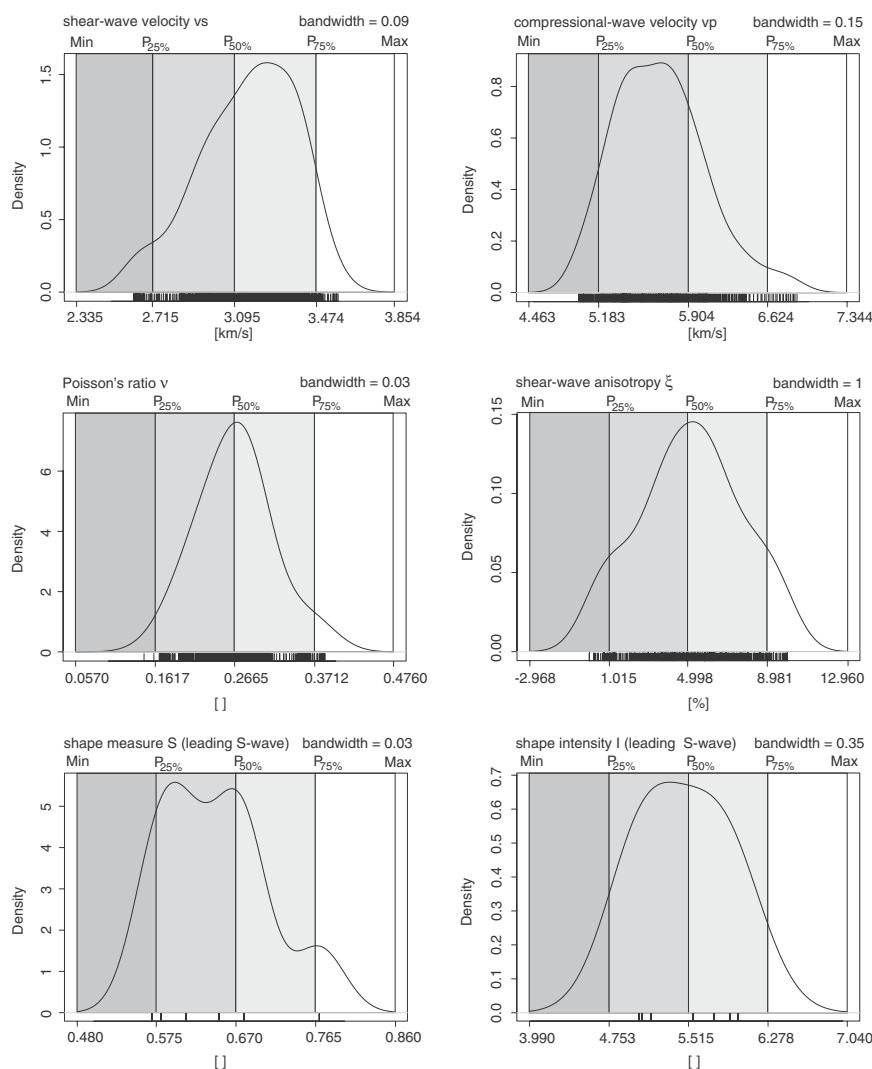


Figure 3 Distribution of the probability densities (kernels) of the six seismic parameters. The linguistic classes are *very low* (black), *low* (dark gray), *high* (light gray), and *very high* (white).



Q into the tunnel, total fracture spacing s_t , fracture persistence p , fracture aperture e , fracture roughness r , fracture infilling f , and schistosity dipping ss . Then, the membership vectors that belong to a cluster are projected onto the Kohonen layer. The cluster labels are also latent (to interpreted) variables. They can also be visualized in the SOM feature maps, but they do not build up the stored information of the SOM feature maps.

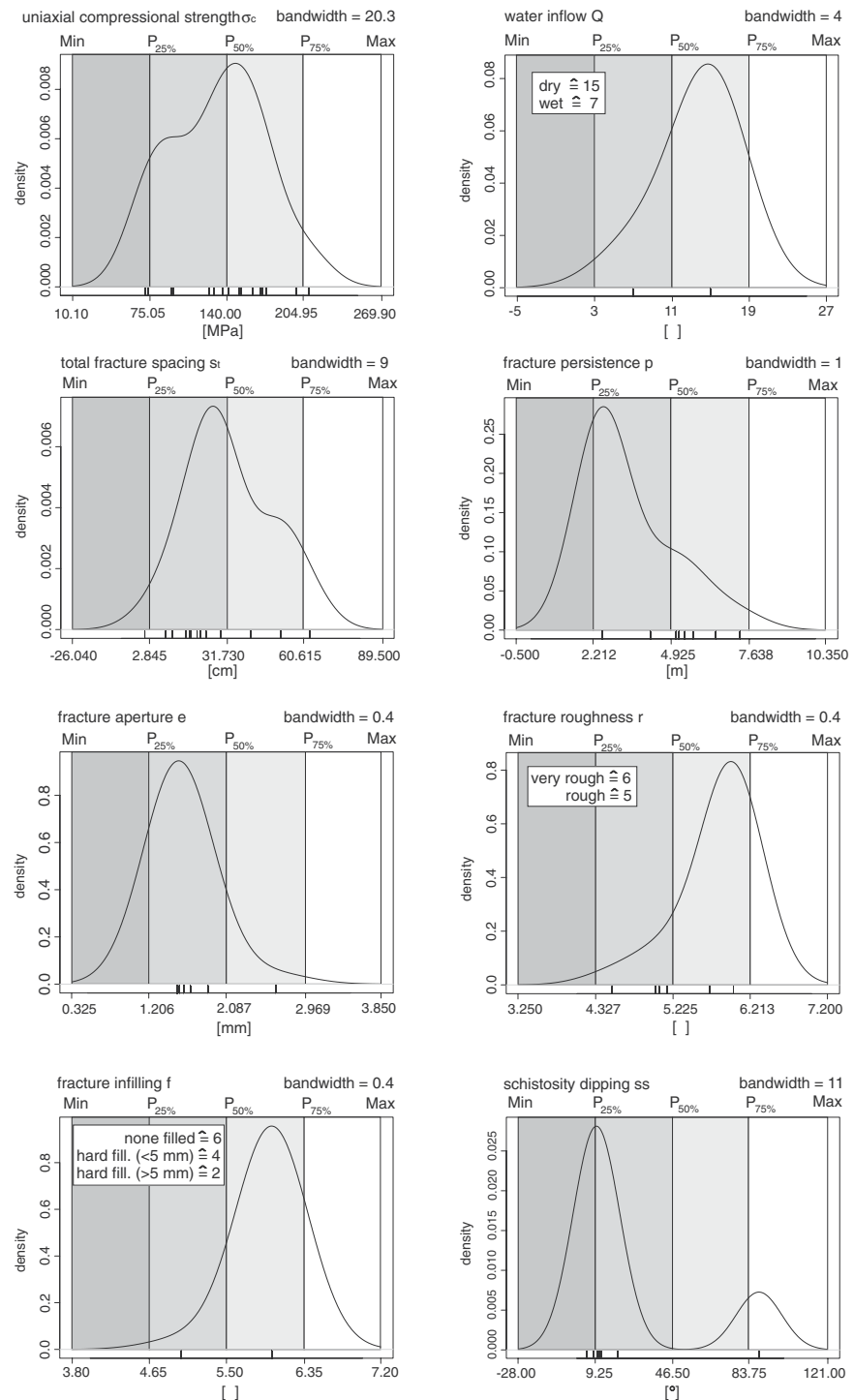
It is assumed that all features are equally important for the clustering. Therefore, each feature is normalized, so that its mean value averaged over the entire feature vectors $\bar{y}_i, i = 1, \dots, 729$ is close to zero [14]. Once all \bar{y} are normalized, they could be partitioned into a preferred number of clusters. Two constrains are formulated to find a representative number of clusters:

- high average quality of separation of all clusters
- high quality of separation of each single cluster

A partitioning method, called *pam* [15, 16], is used to separate k clusters of the 14-dimensional feature space. The clusters are constructed by assigning each feature vector to the nearest cluster. The goal of *pam* is to find k representants (cluster mean values) that minimize the sum of the dissimilarities of the vectors to their closest representant. A silhouette width $s(i)$ is determined as an indicator for the separation quality of every $\bar{y}(i)$. The *pam* algorithm can be summarized as follows:

- Calculate the average dissimilarity $a(i)$ between $\bar{y}(i)$ and all other vectors of a cluster to which $\bar{y}(i)$ belongs.
- Calculate for all other clusters C the average dissimilarity $d(i, C)$ of $\bar{y}(i)$ with respect to all vectors of C .
- The smallest of these $d(i, C)$ becomes $b(i) = \min_C d(i, C)$. It can be seen as the dissimilarity between

Figure 4 Distribution of the probability densities (kernels) of the eight geological parameters. The linguistic classes are *very low* (black), *low* (dark gray), *high* (light gray), and *very high* (white). Q , r , and f can only be subjectively measured [11].



$\vec{y}(i)$ and its *neighbour* cluster, i.e., the nearest cluster to which it does not belong.

- Finally, calculate the silhouette width $s(i) = \frac{b(i) - a(i)}{\max(a(i), b(i))}$, as an indicator for the separation quality of a $\vec{y}(i)$.

Feature vectors with a large $s(i)$ (almost 1) are very well separated, a small $s(i)$ (around 0) means that the observation lies between two clusters, and observations with a negative $s(i)$ are probably placed in a wrong cluster.

3. Results and discussion

3.1. Seismic and geological features

First, each seismic feature is visualized within the Kohonen layer (Figure 5) by its semi-quantitative class values (see Section 2.2). The class distributions of v_p , v_s , and v (v is a function of v_p and v_s) and of S and I have more or less a similar shape, whereas the shape of the ξ image is very different. Classes of a single feature, subjectively and logically defined, describe the data manifold in-

dependently from other features as single component planes.

Further, each geological feature is also visualized as a function of all combined seismic features within the SOM (Figure 6). The following geological features are mapped: uniaxial compressive strength of the rock σ_c , water flow Q into the tunnel, total fracture spacing s_t , fracture persistence p , fracture aperture e , fracture roughness r , fracture infilling f , and schistosity dipping ss . Each geological feature map can be described by all seismic features within the SOM, whereby the overview

Figure 5 SOM mapping results in the Kohonen lattice based on the six seismic feature classes. Areas are labeled such as vp_2^l , consisting of the name of the variable (vp), the superscript with name of the class (l , low), and the subscript with the number of this area (2). The classes are derived from quantiles of the probability density distributions (Figure 3): v.l., very low (black); l., low (dark gray); h., high (light gray); and v.h., very high (white).

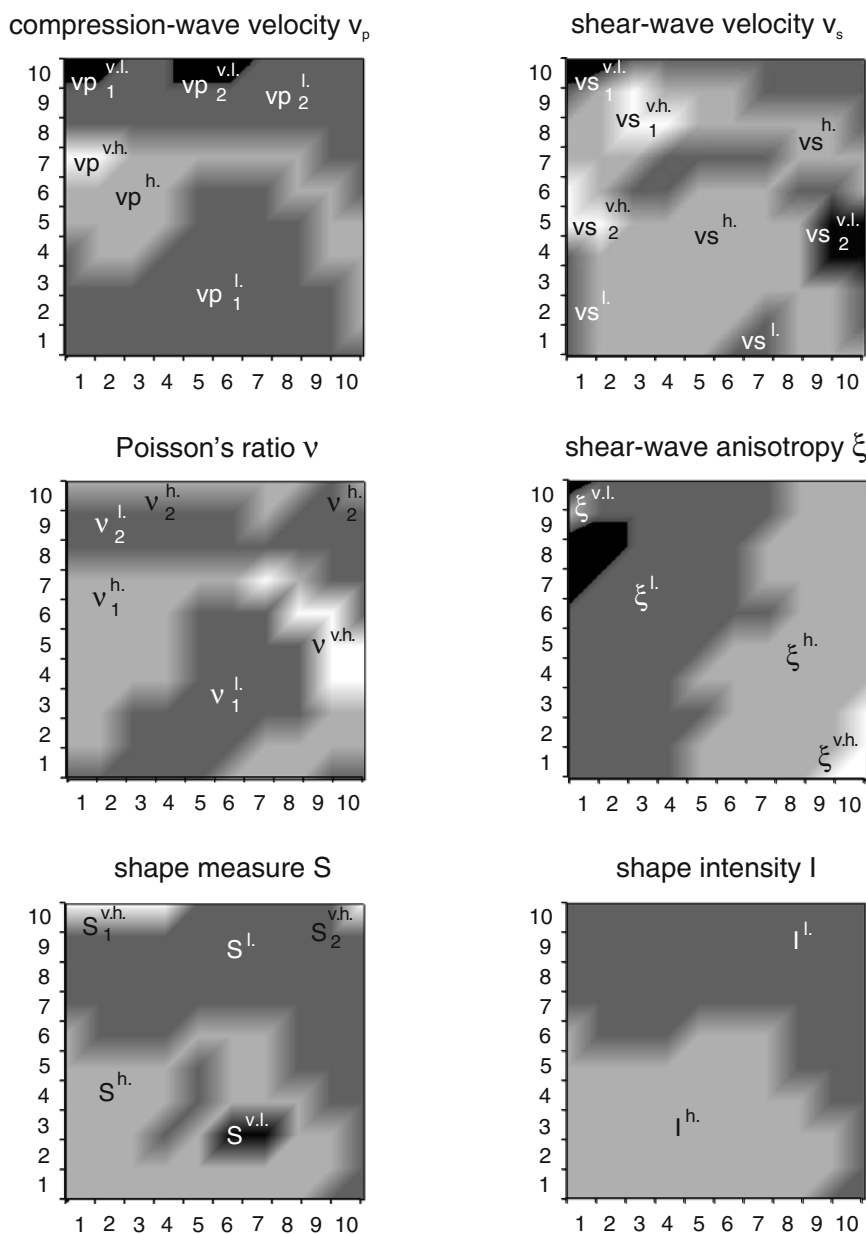
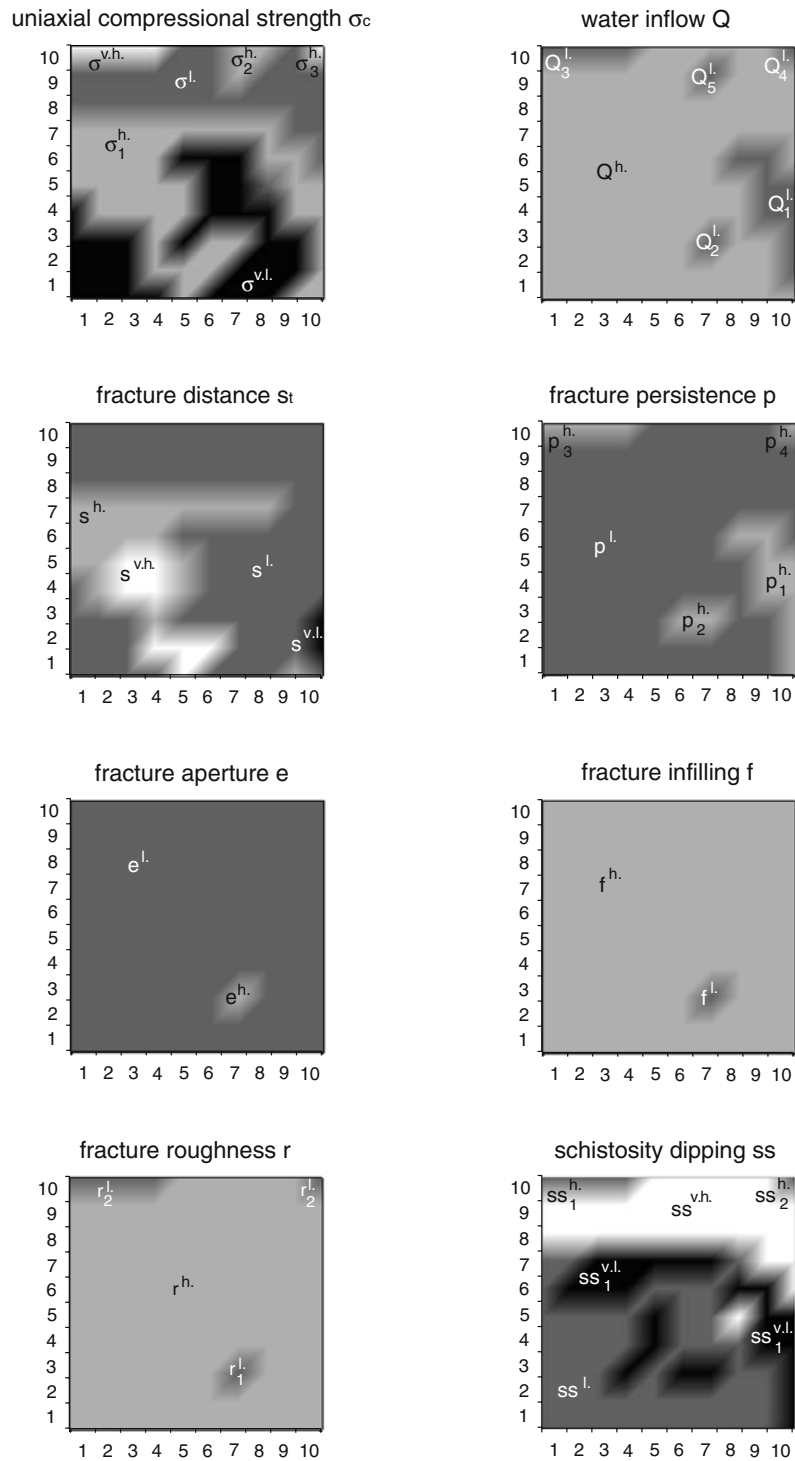


Figure 6 SOM mapping results of geological features in the Kohonen lattice (10×10 neurons). Areas are labeled such as σ_1^h , consisting of the name of the variable (σ), the superscript with name of the class (*h.*, high), and the subscript with the number of this area (1). The classes are derived from Figure 4: v.l., very low (*black*); l., low (*dark gray*); h., high (*light gray*); and v.h., very high (*white*).



of the features is remained. Some of the geological feature maps (e.g., σ) have similar class distributions like the seismic features (e.g., vp).

Different states of a geophysical feature should describe different geological situations in the rock mass. For example, the neurons in the SOM image (Figure 5)

with lattice coordinates (1–2, 10) and (9–10, 4–5) describe two different geophysical situations because the neurons are distant within the image (see property 2 in Section 2.1). Significant geological features are also different in these regions such as rock fracturing s_t , fracture length p , and water inflow Q (Figure 6). The

main reason for the different seismic patterns is that both rock mass regions show brittle deformed fault zones of different tectonic genesis and geometry [1, 17].

Table 1 shows average differences between these regions comparing clusters 2 and 9. Thus, both rock mass regions can be described, and the overview of the complete multidimensional feature space is guaranteed. For example, the heterogeneous distribution of Poisson’s ratio ν (Figure 5) shows that the influence of ν_S dominates for *very low* ν_S values. The influence of ν_P to the ν values dominates for *high to very high* ν_P values. The fracture distance s_t and the existence of water Q are responsible for the seismic feature vectors. This result confirms theoretical analyses of [5, 6] that for dry rock, the P-wave velocity decreases more rapidly with the crack density than the S-wave velocity; in contrast, for a completely saturated rock, ν_S and ν_P decrease uniformly with the crack density, but ν_S initially decreases about twice as fast than ν_P . Interpretations based on correlations would be prone to discover this result under in situ conditions. Correlation coefficients between the features are very small, e.g., $Corr(\nu_P, Q) = 0.21$, $Corr(\nu_S, Q) = 0.57$, $Corr(\nu, Q) = -0.30$, $Corr(\nu_P, s_t) = 0.38$, $Corr(\nu_S, s_t) = 0.52$, and $Corr(\nu_P, s_t) = -0.15$. Another example shows that feature maps of the fracture length p and of the water existence Q (Figure 6) have physically reliable relationships. Long fractures rise the hydraulic conductivity and hence the water flow into the tunnel. The feature maps between p and Q show this relationship very well, whereby both images were independently generated by

the SOM network, which is, again, only based on the geophysical features.

3.2. Multidimensional feature clusters

Another way to get access to the multidimensional feature space is to project clusters onto the Kohonen layer (see Section 2.3). Clusters, derived from objective partitioning methods, describe homogeneous units in the data manifold of all combined features.

Active neurons (black) are plotted for each cluster within the SOM (Figure 7). Feature vectors of similar clusters are related to active neurons in similar SOM regions. Active neuron areas of each cluster are polymorphic-shaped and have partially dispersed distributions with small overlaps. But they are still separated from regions of other clusters. Some clusters show the same arc-shaped structures like the feature maps based on single classes (Figures 5 and 6).

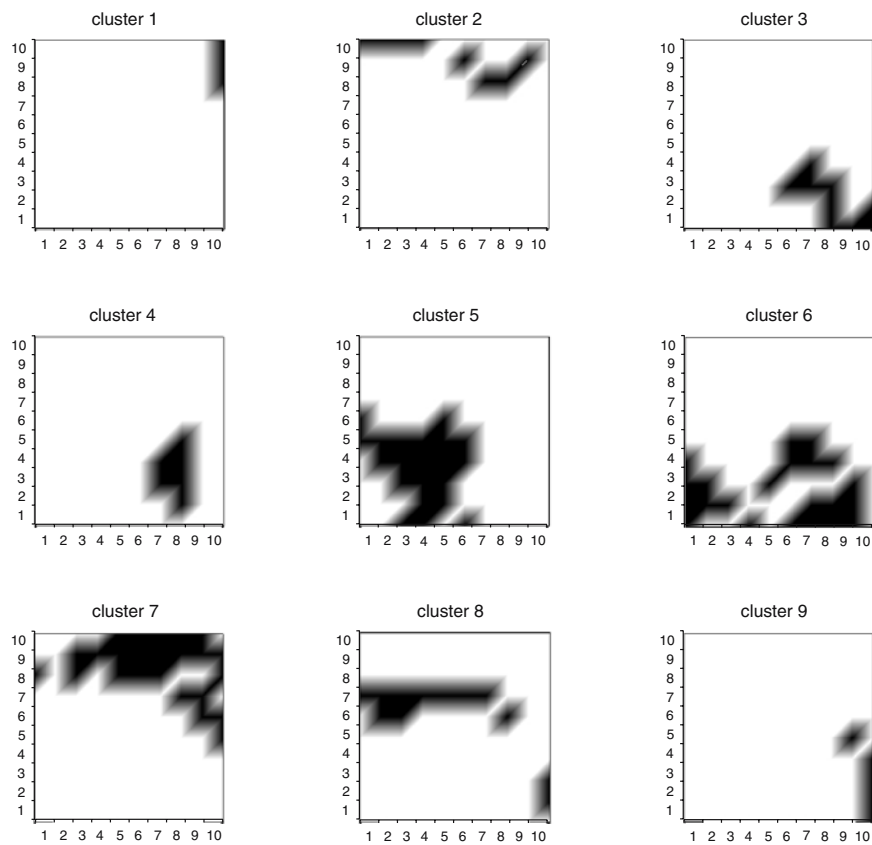
The number of clusters depends on the observer’s subjectivity (precision), the interpretation overview, and the separation quality of the clusters. There is no objective number of clusters to describe the data manifold as best as possible (author’s opinion). Generally, with an increasing cluster number ($k \rightarrow 729$), the precision and the separation quality increase, whereas the overview decreases. When the number of clusters becomes too large, the overview of the clusters gets lost. The separation quality is given by the silhouette width (Figure 8). The average and the minimum cluster silhouette width increase strongly until the number of

Table 1 Homogeneous rock mass units to describe the rock mass quantitatively by using all seismic and all geological features in combination.

	1	2	3	4	5	6	7	8	9
$\nu_P (\frac{km}{s})$	5.36	5.19	5.37	5.65	5.81	5.60	5.32	6.65	6.03
$\nu_S (\frac{km}{s})$	2.93	2.83	3.20	3.35	3.37	3.07	3.17	3.16	2.72
ν ()	0.286	0.288	0.225	0.228	0.245	0.286	0.225	0.354	0.372
ξ (%)	6.2	1.7	8.0	6.6	3.7	3.0	4.9	3.2	8.8
S ()	0.77	0.77	0.57	0.57	0.65	0.68	0.61	0.58	0.58
I ()	5.04	5.04	5.56	5.56	5.99	5.76	5.07	5.16	5.16
σ_c (MPa)	209	209	170	173	162	71	93	168	162
Q ()	dry	wet	dry	dry	dry	dry	dry	dry	wet
s_t (cm)	21.8	11.0	29.2	17.6	51.5	29.2	29.2	51.6	0.6
p (m)	4.2	5.2	5.1	7.4	2.5	2.5	2.5	2.5	6.5
e (mm)	1.60	1.55	1.53	2.65	1.53	1.53	1.53	1.53	1.88
r ()	rough	rough	rough	rough	very r.	very r.	very r.	very r.	very r.
f ()	no	no	no	hard	no	no	no	no	no
ss (°)	10	10	5	5	8	20	88	12	8

The nine clusters are represented by the 14 mean values. Figures 3 and 4 show the semantic understanding of the parameters, especially for the ordinal variables Q , r , and f .

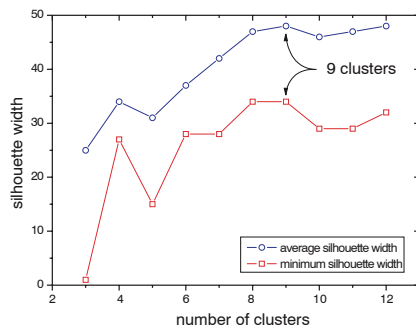
Figure 7 SOM classification results based on nine homogeneous seismic–geological rock mass units (clusters). Neurons become active (*black*) within the SOM when the seismic feature vectors, which belong to one of the units, stimulate the Kohonen lattice. The *white areas* exemplify inactive regions, and the *gray boundaries* result from imaging process. General characteristics of the homogeneous rock mass units (Table 1) can be seen in the feature maps: *distant black areas* represent differences between the clusters.



clusters is nine. The average silhouette width is nearly stable for more than nine clusters, whereas the minimum silhouette width decreases slightly. Thus, a cluster number of nine is preferred (Table 1). It can be seen that some feature mean values of different clusters remain nearly unchanged. Hence, their influence to the separation is less important.

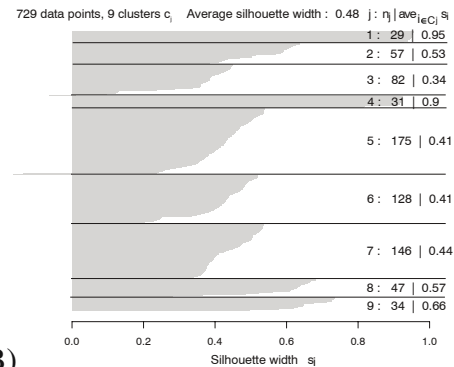
3.3. Application of a SOM network

A trained SOM network as discussed above was applied to a new tunnel segment of the multifunction station of the Gotthard base tunnel (Switzerland) at the intersection with the Faido tunnel, where large instabilities related to a large fault zone occurred. Seismic



A)

Figure 8 Silhouette width s as a function of the cluster number j with $s \cdot 100\%$ is illustrated in (A). The average silhouette width $ave_{C_j} s$ of all clusters, the minimum silhouette width $mini_{i \in C_j} s_i$ of a single cluster, and a representative number of clusters to diversify the seismic–geological feature space are shown (A).



B)

Nine clusters (see Table 1) represent the feature space well. (B) The clustering result: the average silhouette width $ave_{i \in C_j} s_i$ of the nine clusters, the number and the plotted s_i of the cluster members, the number of the cluster members, and the silhouette width s_i of each cluster.

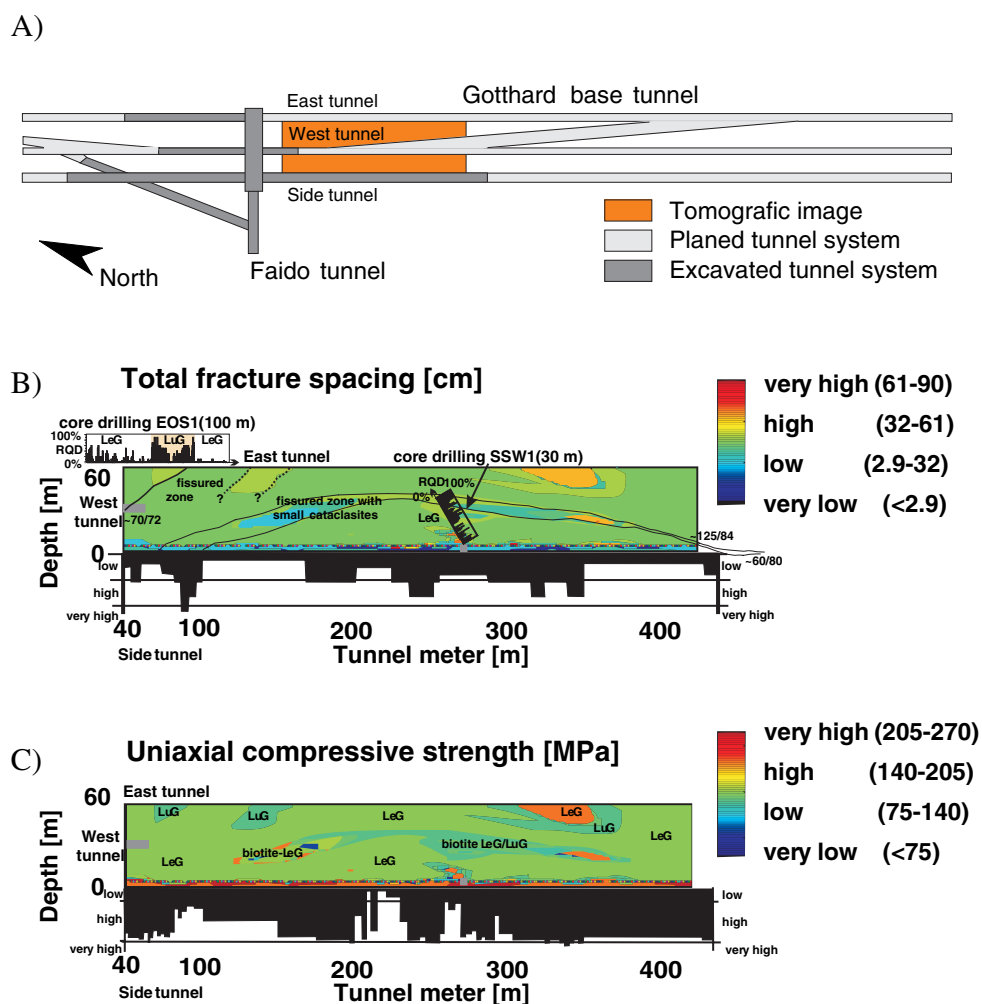
investigations were used to characterize the local geological conditions within the non-excavated west and east tunnels (Figure 9A). These investigations consisted of a single 400×60 m tomographic image generated in the so-called side tunnel south of the Faido adit.

First, a SOM network was trained (Figure 2) with the seismic attributes v_P , v_S , and v of the tomographic images from the Faido tunnel and applied to the new data set resulting from the 400×60 m tomographic image. The other three seismic features ξ , S , and I were neglected due to practical reasons and time constraints imposed from the ongoing construction works. In a second step, two engineering geological parameters, the total fracture spacing s_t (Figure 9B) and the uniaxial compressive strength σ_c (Figure 9C), were predicted within the extension of the tomographic plane.

It should be noticed that all images contain class values (“very low,” “low,” “high,” and “very high”). The

labels (i.e., LeG, LuG, fissured, or cataclasites) within the images show further descriptions of the geological conditions (rock mass units), which are similar to those in the Faido tunnel. The black lines in Figure 9B describe significant geological boundaries. On the image edges, these boundaries represent the interpretation results of the prediction together with the geological mapping, which were outlined in a later excavation stage. That means the predicted engineering geological properties could be directly compared to fracture spacings and rock mass strengths from tunnel wall mapping (tunnels west and east) and additionally from core drilling results (Figure 9B). For example, the 30-m-long core drilling SSW1 (Figure 9B) confirmed the prediction of s_t in the centre of the tomographic image. The 100-m-long core drilling EOS1 (Figure 9) also confirmed the prediction of s_t and σ_c in the upper left part of the tomographic image.

Figure 9 Interpretation results of a tomographic image (400×60 m) in the Gotthard base tunnel (A). A SOM network trained with the seismic data, based only on v_P , v_S , and v from the Faido tunnel, was applied to the new seismic data set. The total fracture spacing s_t (B) and the uniaxial compressive strength σ_c (C) were predicted as class labels (intervals). The labels (i.e., LeG, LuG) within the images show the gneiss varieties similar to data along the Faido tunnel. The added black lines describe significant boundaries. The predicted spatial distribution of s_t and σ_c corresponds well with the geological data of the drill cores (EOS1, SSW1) and with the mapping results of s_t , σ_c , and ss along the side tunnel.



4. Conclusion

Several reasons exist why conventional interpretation methods such as correlations are limited to characterize geophysical and/or geological in situ data of higher dimensionality.

- Each geophysical feature is a realization (function) of the multidimensional geological feature space because the rock mass is given and the geophysical data result from geological conditions. Interpretations become difficult, due to ambiguous interpretation results, because geophysical interpretations are always done the other way around (conclusions from geophysical to geological features).
- High noise of geophysical data mainly due to varying in situ conditions.
- Complexity and non-linearity between geophysical and geological features.

Pairwise correlations show relationships between two features; they do not show the total amount of information of the observed feature spaces. Complicated distributions of features within the maps exemplify the complexity and non-linearity of the multidimensional feature spaces.

Interpretations based on feature classes are advantageous if detailed relationships between single features are of interest (see Section 3.1). Nevertheless, they can lead to complicated classification schemes such as for the fracture spacing s_t :

s_t is very low if v_S is very low or ξ is very high.

s_t is low if v_P is low and v is low and ξ is low or high.

s_t is high if v_P is high and very high and v is high.

s_t is very high if v_P is high or v_S is high.

For general analyses from a global perspective, SOM interpretations should base on feature clusters (see Section 3.2). The feature maps based on clusters (Figure 7 and Table 1) show similarities and differences of the clusters with respect to the complete geophysical–geological feature space. The cluster mean values exemplify which features are responsible for the characteristics of the clusters.

It could be shown that it is possible to characterize geological rock mass properties from interpretations of multidimensional geophysical (seismic) in situ data. The classifications are automatically performed by an SOM. This method is based on neural information processing and is more powerful compared to conventional methods, such as correlations and spatial profile descriptions. The reason is that all seismic features are jointly used for the classification. The interrelationships of the geo-

physical features as well as their relationships to the geological features are visualized in two-dimensional maps. Complicated distributions of features within the maps exemplify the complexity and non-linearity of the multidimensional feature spaces. These feature maps can be visually described and easily interpreted. Hence, the overview of all features and all relationships can be retained for each interpretation.

Classifications are performed in an automated way, which is helpful for online predictions of geological conditions in undiscovered rock mass regions (e.g., during underground mining processes). Even if geological data are qualitatively and quantitatively low or the geophysical data are numerically limited, interpretations can still be performed with good results, when all seismic features are used simultaneously. For interpretations of geophysical in situ measurements, the quantity (dimensionality) of the involved features is more important than the quantity and precision of the measurements.

References

1. Klose, C.D.: Engineering geological rock mass characterisation of granitic gneisses based on seismic in-situ measurements, Scientific Technical Report, *GeoForschungsZentrum, Potsdam* (2004). STR 04/08, <http://www.gfz-potsdam.de/bib/pub/str0408/0408.htm>
2. Ji, S., Salisbury, M.: Shear-wave velocities, anisotropy and splitting in high-grade mylonites. *Tectonophysics* **221**, 453–473 (1993)
3. Garbin, H.D., Knopoff, L.: The compressional modulus of a material permeated by a random distribution of circular cracks. *Q. Appl. Math.* **30**, 453–464 (1973)
4. Garbin, H.D., Knopoff, L.: The shear modulus of a material permeated by a random distribution of free circular cracks. *Q. Appl. Math.* **33**, 296–300 (1975)
5. O'Connell, R.J., Budianski, B.: Seismic velocities in dry and saturated cracked solids. *J. Geophys. Res.* **79**(35), 5412–5426 (1974)
6. Henyey, T.H., Pomphrey, R.J.: Self-consistent moduli of a cracked soil. *Geophys. Res. Lett.* **9**, 903–906 (1982)
7. Moos, D., Zoback, M.D.: In situ studies of velocity in fractured crystalline rocks. *J. Geophys. Res.* **88**(B3), 2345–2358 (1983)
8. Stierman, D.J.: Geophysical and geological evidence for fracturing, water circulation and chemical alteration in granitic rocks adjacent to major strike slip faults. *J. Geophys. Res.* **89**(B7), 5849–5857 (1984)
9. Kohonen, T.: Self-organizing formation of topologically correct feature maps. *Biol. Cybern.* **43**(1), 59–69 (1982)
10. Kohonen, T.: *Self-Organizing Maps*, 3rd edition. Springer, Berlin (2001)
11. Bieniawski, Z.T.: *Engineering Rock Mass Classification*. Wiley, New York (1989)
12. Vesanto, J.: *Data Exploration Process Based on Self-Organizing Map*. PhD thesis, Helsinki University of Technology (2002) <http://lib.tkk.fi/Diss/2002/isbn9512258978/>
13. Silverman, B.W.: *Density Estimation*. London (1986)

14. LeCun, Y.: Effective Learning and Second-order Methods, A Tutorial at NIPS 93. Denver (1993)
15. Rousseeuw, P.J.: Silhouettes: a graphical aid to the interpretation and validation of cluster analysis. *J. Comput. Appl. Math.* **20**, 53–65 (1987)
16. Kaufman, L., Rousseeuw, P.J.: *Finding Groups in Data: An Introduction to Cluster Analysis*. John Wiley & Sons Inc., New York (1990)
17. Klose, C.D., Loew, S.: Engineering geological rock mass characterisation of granitic gneisses based on seismic in-situ measurements during tunnel excavations. In: Schubert, W. (ed.) *Rock Engineering Theory and Practice, ISRM Regional Symposium EUROCK '04*, pp. 120–126. VGE (2004)